# Coherent UWB Ranging in the presence of Multiuser Interference

Vinod Kristem, Andreas F. Molisch, *Fellow, IEEE*, S. Niranjayan, *Member, IEEE*, Seun Sangodoyin, *Student Member, IEEE*

***Abstract*—Roundtrip Time-of-arrival (ToA) measurements employing ultra-wideband (UWB) signals can provide high-precision ranging information. However, the accuracy is degraded by multiuser interference (MUI), in particular in the presence of multipath propagation. While the processing gain of time-hopping impulse radio (TH-IR) can be used to suppress the MUI, this is often insufficient. We propose instead a nonlinear processing scheme of TH-IR that effectively suppresses MUI without requiring knowledge of the time-hopping sequences of the interfering users. The principle is that multipath components (MPCs) of interferers do not align closely, for the majority of transmission frames, with the MPCs of the desired signal. Through a judicious choice of algorithm parameters we show that our algorithm is superior to existing (realizable) thresholding and median filter algorithms, and in some cases can even beat genie-aided thresholding algorithms. The performance is robust to both strength and number of the interferers. The results are validated with both standardized 802.15.4a channel models and measured outdoor UWB channels.**

***Index Terms*—Ranging, time-of-arrival, multiuser interference, ultra-wideband**

## I. Introduction

Accurate position information is of high importance in many commercial, public safety, and military applications. While Global Positioning System (GPS) serves this purpose in outdoor environments, it is often unreliable or inaccessible in cluttered environments such as indoors, narrow street canyons, caves, and dense forests. For this reason, alternative positioning techniques based on ranging between ground-based devices need to be explored. While fingerprinting of received signal strength (RSS) has received great attention [3], [4], the ranging accuracy depends on access to database of RSS. Ranging using the ultra-wideband (UWB) signals is promising due to the good range resolution associated with large bandwidth.

Ranging techniques are based on time-of-arrival (ToA) of the first path. ToA estimation is mainly affected by receiver noise, multipath propagation and interference. In a dense multipath channel, the first path is not always the strongest path thereby making ToA estimation challenging.

UWB ranging in the presence of noise and multipath propagation has been studied extensively in the literature. For a single path additive white Gaussian noise (AWGN) channels, a matched-filtering (MF) receiver is the maximum likelihood (ML) ToA estimator with theoretical bounds on the ranging error given in [11]–[13]. For AWGN with multipath, [14] and [15] respectively derived the Cramer-Rao bound (CRB) and Ziv-Zakai bound (ZZB) on the mean square error (MSE) in ToA estimation. The ML estimators for the ToA estimation were proposed in [16] and [17]; however, computational complexity of these estimators limits their implementation. Practical sub-optimal ToA estimators were proposed in [18], [19]. Several low complexity, subsampling ToA estimators, based on the energy-detection (ED) have been proposed in [19]–[21]. The performance of the MF and ED receivers has been summarized in [22]. A two-step hybrid ToA estimator was proposed in [23]. In it, the coarse estimate is obtained from energy detection and a fine estimate is obtained from matched-filtering. A blind, ToA estimator based on model selection by information theoretic criteria is proposed in [24].

Very few papers in the literature addressed the issue of interference in UWB ranging. In multiuser network, signals from multiple users can interfere with the desired signal thereby deteriorating the ranging accuracy. While using distinct time-hopping (TH) sequences for different users, followed by coherent combining of signals can suppress the interference to certain extent, the residual interference can be significant compared to the first arriving path from the desired user, and hence can result in early false alarms. This is because the first arriving path is not always the strongest path. In fact, it can have significantly lower energy than the strongest path, especially in non-line of sight (NLOS) conditions. Thus this effect might occur even in the absence of near/far effects that are the reason for significant MUI in TH communication systems. Hence, finding a good threshold to separate the interference multipath components (MPC) from the first MPC of the desired user is difficult or even impossible.

Ref. [25] proposed non-linear filtering schemes like minimum filtering and median filtering to mitigate the multiuser interference (MUI). Ref. [26] considered both MUI and narrowband interference (NBI), and proposed differential filtering, to mitigate the interference. These papers considered the ED receivers and studied the performance with only one interfering user. While the ED receivers have low cost implementation, its performance is poor compared to matched-filtering (coherent) receivers, especially when the signal-to-noise ratio (SNR) is small. Also, the energy based non-linear filtering schemes cannot exploit noise averaging across frames, as the noise becomes correlated after filtering. MUI mitiga-

The authors are with the Dept. of Electrical Eng. at the Univ. of Southern California, CA, USA.

Emails: kristem@usc.edu, molisch@usc.edu, niranjay@usc.edu, sangodoy@usc.edu

This work is partially supported by the Office of Naval Research (ONR) and Defense University Research Instrumentation Program (DURIP).

A part of this work will appear in Intl. Conf. on Commun. (ICC), 2014.

tion in UWB ranging using coherent receivers is considered in [27]. However, it was assumed that the receiver knows the TH sequences of all the interfering users, and proposed an iterative successive interference cancellation technique for ToA estimation. In a dense multipath channel, this approach becomes computationally intense. More importantly, acquiring the TH sequences of all the interfering users is difficult especially when the users are mobile. It can also happen that the interfering users are hostile and do not share their TH sequences.

The key contributions of the paper are

- *A novel coherent ranging algorithm that suppresses the MUI without having to know the TH sequences of the interfering users.* Only the TH sequence of the desired user is known to the receiver. To the best of our knowledge, this is the first paper in the literature that talks about the MUI suppression for coherent UWB ranging, without having to know the TH sequences of the interfering users. We make use of the fact that after de-hopping the received signal, the receiver effectively has multiple waveforms, one per every frame duration in the TH signal. While the signal MPCs in these waveforms are time-aligned, because of the time-hopping nature, an interference MPC hops around the signal MPCs across different waveforms, thereby making it feasible to separate an interference MPC from a signal MPC.
- *Performance bounds:* We model the MPC delays by a Poisson process and develop bounds on the false alarm probability from interference and noise MPCs and detection probability of signal MPCs, as a function of algorithm parameters.
- We provide a judicious choice of parameters and using the analytical expressions derived earlier, we show that the proposed algorithm effectively suppresses the strongly interfering MPCs.
- *Performance evaluation with synthetic channels:* Using IEEE 802.15.4a channel models, we show that the proposed ranging scheme is robust to the strength of interference and the number of interfering users in the system, and performs much better than the thresholding schemes and the non-linear filtering schemes considered in the literature.
- *Experimental study of performance:* We also carried out an urban outdoor channel measurement campaign with UWB channel sounder and tested the performance of our algorithm in both LOS and NLOS measured scenarios. We compare the performance of our ranging scheme with some well-known coherent and non-coherent thresholding schemes.

The paper is organized as follows. The system model is developed in Sec. II. The thresholding schemes and the proposed ranging algorithm are described in Sec. III-A and III-B respectively. The performance bounds for the proposed ranging scheme are developed in Sec. IV. The performance evaluation is done with synthetic channels in Sec. V. The measurements description and the corresponding results are given in Sec. VI. Finally, the paper is concluded in Sec. VII. The mathematical details are moved to the Appendix.

## II. System Model

We consider a multiuser network with $(I+1)$ users simultaneously transmitting at any given time. Without loss of generality, we assume the first user as desired and the other $I$ users as interference. The users are assigned fixed and distinct TH sequences. The TH signal transmitted by the $i^{\text{th}}$ user is given by [6]

$$s_i(t) = \sqrt{E_i}\sum_{n=1}^{N} p(t-(n-1)T_f-c_i(n)T_c-D_i),\ 0 \le t \le NT_f,$$

where $p(t)$ is the unit energy UWB pulse, $E_i$ is the signal energy per frame, and $c_i$ is the chip sequence of the $i^{\text{th}}$ user with $c_i \in \{0,1,\cdots,N_c-1\}^{N_c}$. $T_c$ is the chip duration, $T_f$ is the frame duration, $N_c$ is the size of the code alphabet and the number of chips per frame ($T_f = N_c T_c$), and $N$ is the number of frames per symbol. $D_i$ is the transmission start time of the $i^{\text{th}}$ user. Without loss of generality, we assume $D_1 = 0$. We assume that all users use the same pulse shape $p(t)$.

Let $h_i(t)$ denote the impulse response of the channel between the $i^{\text{th}}$ user and the receiver. The received signal is given by [1]

$$r(t) = \sum_{i=1}^{I+1} s_i(t) * h_i(t) + n(t), \tag{1}$$

where $(*)$ is the convolution operation and $n(t)$ is the zero-mean AWGN with variance $N_0$. The model implicitly assumes that the channel is quasi-static during the transmission of the ranging signals, given typical pedestrian coherence times ($\sim$ 10 ms [1]), this is a realistic assumption. We assume that NBI can be removed by notch filtering and hence do not model it.

The signal-to-noise ratio (SNR) and signal-to-interference ratio (SIR) for the desired user are defined as follows

$$\text{SNR} \triangleq \frac{E_1}{N_0},\ \text{SIR}(i) \triangleq \frac{E_1}{E_{i+1}},\ i = 1,2,\cdots,I. \tag{2}$$

Notice that SIR in general is a function of user index as different interfering users can transmit with different power and can be at different distances from the receiver. We assume that the receiver only knows the TH sequence of the desired user and not of the interfering users. The receiver can now perform the de-hopping process, by dividing the observation time into $N$ intervals, $I_n \triangleq [c_1(n)T_c+(n-1)T_f,\ c_1(n)T_c+(n-1)T_f+T], 1 \le n \le N$, each of length $T (T < T_f)$. We assume that the delay spread of the channel is smaller than one frame duration. Without loss of generality, we assume that the chip-sequence for the desired user is the all zero sequence.

The receiver effectively has the following $N$ waveforms

$$r_n(t) \triangleq r(t+(n-1)T_f),\quad 1 \le n \le N,\ 0 \le t \le T \tag{3}$$

$$= S(t) + I_n(t) + N_n(t), \tag{4}$$

[1]The frames from different users can arrive at different times and is implicitly captured by the channel impulse response of the users. The delay corresponding to the first MPC can be different for different users.

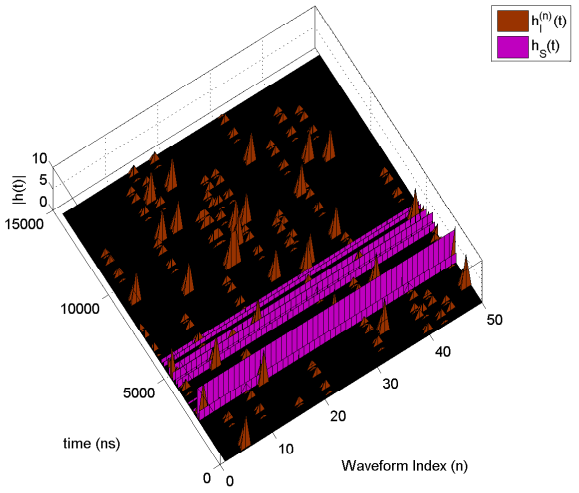


Fig. 1. Effective impulse responses after de-hopping. (IEEE 802.15.4a CM1 channel realization with $N = 50$ and $I = 1$.)

where the signal, interference and the noise terms are defined as follows:

$$S(t) \triangleq \sqrt{E_1}p(t) * h_1(t) = p(t) * h_S(t), \quad (5)$$

$$I_n(t) \triangleq \sum_{i=2}^{I+1} \sqrt{E_i}p(t) * h_i\left(t - c_i(n)T_c - D_i\right) = p(t) * h_I^{(n)}(t), \quad (6)$$

$$N_n(t) \triangleq n(t + (n-1)T_f), \quad (7)$$

where $h_S(t) \triangleq \sqrt{E_1}h_1(t)$ is the effective impulse response between the desired user and the receiver and $h_I^{(n)}(t) \triangleq \sum_{i=2}^{I+1} \sqrt{E_i}h\left(t - c_i(n)T_c - D_i\right)$ is the effective impulse response between the interfering users and the receiver. $N_n(t)$ is a Gaussian process with the same statistics as $n(t)$.

Notice that while $h_S(t)$ is same for all the $N$ waveforms, $h_I^{(n)}(t)$ is different for different waveforms. This is because the chip sequence $c_i(n)$ is different for different $n$. Figure 1 compares the sample impulse responses $h_S(t)$ and $h_I^{(n)}(t)$ for different $n$. It can be seen that the desired signal MPCs, across the $N$ waveforms, are time aligned and have the same strength. The interference MPCs appear to be time-hopping across the different waveforms. Hence, it is possible to separate the signal MPC from the interference MPC without even knowing the TH sequences of the interfering users.

## III. ToA estimation algorithms

Our goal is to extract the ToA of the first path for the desired user, from the waveforms $\{r_n(t)\}_{n=1}^N$. We first briefly discuss some ToA estimation schemes developed in the literature for mitigating the MUI and then describe the proposed ToA estimation algorithm.

Since the high-resolution CLEAN algorithm is a base for these ranging schemes, we briefly describe it below.

*CLEAN algorithm:* It is used to extract the MPCs from the received waveform. CLEAN is an iterative deconvolution technique first introduced in [7] for the enhancement of the radio astronomical maps of the sky and widely used in microwave and UWB communities as an effective post-processing method for time-domain channel measurements [8], [9]. In it, the received signal is correlated with the template signal, and the amplitude and location of the correlation peak is determined, followed by a subtraction of the contribution of the thus-detected MPC from the received signal.

For instance, if $y(t) = \sum_{k=1}^{L} \alpha_k p(t - \tau_k) + n(t)$ is the received signal with $p(t)$ being the template signal, the correlation is given by

$$\rho(\tau) = \int p(t-\tau)^* y(t)dt = \sum_{k=1}^{L} \alpha_k R_p(\tau - \tau_k) + N(\tau), \quad (8)$$

where $R_p(.)$ is the auto-correlation of the template signal and $N(\tau) \triangleq \int p(t-\tau)^* n(t)dt$ is a circular symmetric complex Gaussian random process with covariance function $K_N(t_1, t_2) = N_0 R_p(t_1 - t_2)$.

The location of the strongest MPC is $\hat{\tau}_1 = \arg\max_\tau |\rho(\tau)|$ and the corresponding strength is $\hat{\alpha}_1 = \rho(\hat{\tau}_1)$. The contribution of the strongest MPC, $\hat{\alpha}_1 p\left(t - \hat{\tau}_1\right)$, is removed from the received waveform. The residual signal is correlated with the template to determine the next strongest MPC. This process repeats and by the end of $M$ iterations, we have the MPCs $\{\hat{\alpha}_1, \cdots, \hat{\alpha}_M, \hat{\tau}_1, \cdots, \hat{\tau}_M\}$, and the residual signal is

$$y^{(M)}(t) \triangleq y(t) - \sum_{k=1}^{M} \hat{\alpha}_k p(t - \hat{\tau}_k). \quad (9)$$

The process stops when the peak correlation between the residual signal and the template falls below a predetermined threshold $\eta\,|\rho_{\max}|$ ($0 \le \eta \le 1$ and $\rho_{\max} \triangleq \hat{\alpha}_1$ is the maximum correlation between the received waveform and the template).

Notice that the estimated MPC location can be off from the true location. When the MPCs are resolvable, the offset in the location estimate is bounded by [22]

$$\mathcal{P}\left(|\tau - \hat{\tau}| \le W\right) = 1 - Q\left(\sqrt{\frac{|\alpha|^2}{N_0}\left(1 - R_p(2W)\right)}\right), \quad (10)$$

where $Q(.)$ is the Q-function, $\alpha$ is the strength of the MPC and $W$ is the window size. Hence, the larger the strength of the MPC and the faster the decay of the auto-correlation of the template signal, the higher the probability that the estimate is within the window $[\tau - W \;\; \tau + W]$.

### A. Thresholding schemes

One simple and commonly used strategy for mitigating the MUI is to average the $N$ waveforms, extract the MPCs from the averaged waveform using CLEAN, use a *good* threshold to separate the first arriving signal MPC from the interference MPCs and the noise peaks, and declare the MPC with the smallest delay as the ToA estimate.

Notice that the ranging error is sensitive to the threshold $\eta$. In the presence of noise and/or MUI, finding a good threshold is challenging. Setting large $\eta$ can result in missing the weak signal MPCs and a small $\eta$ can result in early false alarms from capturing interference MPCs or noise peaks.

Averaging works well when $N$ is very large or SIR is high. But in reality, $N$ is limited by the coherence time of the

channel. Since all users transmit with similar power level, SIR of 0 dB is typical and it can even attain a large negative value due to near/far effects or LOS/NLOS situations. For a finite $N$ and a reasonable SIR, the residual interference after averaging can be comparable to or larger than the first arriving MPC from the desired user. Hence, this approach can result in large miss-detection and early false alarms, thereby deteriorating the ranging accuracy.

In the remainder of the paper two different thresholds are considered as benchmarks:

*1) Genie thresholding:* For every channel realization, $\eta$ is chosen to minimize the instantaneous ranging error. This is done by performing the brute-force Monte Carlo simulations-based search. Note that this is not feasible in practice: in order to determine the instantaneous ranging error and hence the optimal $\eta$, we would have to know the instantaneous channel impulse response which is the quantity we wish to measure.

*2) Lookup table based thresholding:* $\eta$ is chosen to minimize the mean-squared error (MSE) in the range estimates. This can be realized in practice by forming a lookup table of optimal $\eta$ for different SNR, SIR, $I$ and $N$. The threshold is picked based on the operating conditions.

### B. Proposed ToA estimation algorithm

By averaging the waveforms, we lose the information about the location of the interference MPCs. Instead, we can first determine the location of interference MPCs, remove their contribution from each of the waveforms and then average the interference-free waveforms and extract the ToA information. The algorithm has been summarized in Algorithm 1. We now describe each of the steps in detail.

*1) Impulse response extraction from the waveforms:* We use CLEAN algorithm to extract the impulse responses from each of the $N$ waveforms. We use a fixed correlation threshold of $\mu \triangleq 2.12\sqrt{N_0}$, so that the false alarm probability due to the noise peak is small. A noise peak occurs at $\tau$ if the correlation exceeds the threshold; the probability of this event is

$$\mathcal{P}\left(|\rho(\tau)| > \mu\right) = \mathcal{P}\left(|N(\tau)| > \mu\right) = \exp\left(-\frac{\mu^2}{N_0}\right) = 0.01.$$

Let $\left\{\hat{\tau}_k^{(n)}, \hat{\alpha}_k^{(n)}, 1 \le k \le L_n\right\}$ be the location and the strength of the MPCs extracted from the waveform $r_n(t)$. The impulse response is defined as $\hat{h}_n(t) \triangleq \sum_{k=1}^{L_n} \hat{\alpha}_k^{(n)} \delta(t - \hat{\tau}_k^{(n)})$. Since $r_n(t)$ has contributions from desired user, interfering users, and noise, the MPC delay $\hat{\tau}_k^{(n)}$ can correspond to desired user or the interfering users or the noise peak.

*2) Separating the interference and signal MPCs:* Consider the set $\left\{\hat{h}_n(\tau), 1 \le n \le N\right\}$. As seen from Figure 1, if $\tau$ corresponds to a signal MPC location, most of the values in the set are similar. If $\tau$ corresponds to a noise peak in one waveform, many of the values in the remainder of the set will be zero since the odds of noise peaks happening at the same location in multiple waveforms are low. If $\tau$ corresponds to an interference MPC location in one waveform, some of the values in the remainder of the set will be zero and even the non-zero values in the set are distinct. This is because an

**Step 1:** Impulse response extraction from waveforms
**for** *n = 1:N* **do**
  MPCs extraction from $r_n(t)$:
  $\left\{\hat{\tau}_k^{(n)}, \hat{\alpha}_k^{(n)}, 1 \le k \le L_n\right\}$
  Impulse response: $\hat{h}_n(t) \triangleq \sum_{k=1}^{L_n} \hat{\alpha}_k^{(n)} \delta(t - \hat{\tau}_k^{(n)})$
**end**
**Step 2:** Separating the interference/noise and signal MPCs
**for** *n = 1:N* **do**
  $\Delta_n^I = [\,]$, $\Delta_n^S = [\,]$
  **for** *k = 1:$L_n$* **do**
    Accumulate MPCs in $2W$ window:
    $X_m \triangleq \int_{w=-W}^{W} \hat{h}_m(\hat{\tau}_k^{(n)} - w)dw$
    Consider the set $\{X_m, 1 \le m \le N\}$.
    **if** $\exists$ *a cluster of at least $\bar{N}$ non-zero data points around $X_k$* **then**
      Declare $\hat{\tau}_k^{(n)}$ as a signal MPC
      Collect signal MPCs: $\Delta_n^S = [\Delta_n^S\ \hat{\tau}_k^{(n)}]$
    **else**
      Declare $\hat{\tau}_k^{(n)}$ as an interference/noise MPC
      Collect interference MPCs: $\Delta_n^I = [\Delta_n^I\ \hat{\tau}_k^{(n)}]$
    **end**
  **end**
**end**
**Step 3:** Interference suppression and noise averaging
**for** *n = 1:N* **do**
  $\tilde{r}_n(t) = r_n(t) - \sum_{\hat{\tau} \in \Delta_n^I} \hat{h}_n(\hat{\tau}) p(t - \hat{\tau})$
**end**
Noise averaging: $r_{\text{avg}}(t) = \frac{1}{N} \sum_{n=1}^{N} \tilde{r}_n(t)$.
**Step 4:** Range (or) ToA estimation
MPC delay extraction from $r_{\text{avg}}(t)$: $\{\hat{\tau}_k, k \ge 1\}$
$\widehat{\text{ToA}} = \min\left\{\hat{\tau}_k : |\hat{\tau}_k - \hat{\tau}_{k+1}| < \frac{5.3}{\lambda}\right\}$.

**Algorithm 1**: Proposed ToA estimation

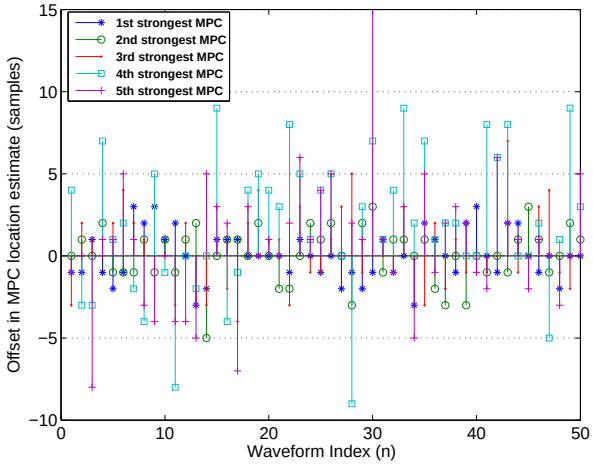


Fig. 2. Error in MPC location estimates obtained using CLEAN, for five strongest MPCs. (IEEE 802.15.4a CM1 channel realization and second derivative of basic Gaussian pulse with pulse width of 1 ns are used. $N = 50$, SNR = 30 dB, sampling time = 25 ps, and $I = 0$.)

interference MPC time-hops across the different waveforms as explained earlier. However, we also have to take into account that because of noise, the estimated MPC locations can vary around their true locations. If $\tau$ is the true signal MPC location, because of $i.i.d.$ noise in different waveforms, the offset in the location estimate is also $i.i.d.$ across the waveforms, but with high probability the estimates will all lie in $[\tau - W, \tau + W]$. This can also be seen from Figure 2, which plots the offset in the signal MPC location estimates for the strongest five MPCs. It can be seen that the amount of offset is inversely proportional to the strength of the MPC.

Using the intuition presented above, we now propose the following heuristic rule to decide if the MPC location $\hat{\tau}_k^{(n)}$ corresponds to a signal MPC or an interference/noise MPC.

For $1 \leq n \leq N$ and $1 \leq k \leq L_n$,

- Construct the set $\{X_n, 1 \leq n \leq N\}$, where $X_n \triangleq \int_{w=-W}^{W} \hat{h}_n(\hat{\tau}_k^{(n)} - w)dw$. This is done to compensate for the offset in the MPC location estimates. Let $M$ be the number of non-zero values in this set.
- $M < \bar{N}$: Declare $\hat{\tau}_k^{(n)}$ as an interference/noise MPC (A signal MPC will be detected in at least $\bar{N}$ out of $N$ waveforms). $\bar{N}$ is an algorithm parameter that will be discussed later.
- $M \geq \bar{N}$: If $\hat{\tau}_k^{(n)}$ is an interference MPC, these $M$ data points are distinct and far apart. If it is a signal MPC, most of these data points are clustered. In some of the waveforms, an interference MPC can overlap with the signal MPC thereby deteriorating the MPC amplitude estimate. Since we do not assume the knowledge of strength of interference MPCs, we simply identify such estimates and discard them as below.
  - Construct a circle of radius $\gamma$ around every data point and count the number of data points enclosed by the circle (including the center).
  - If there is no such circle enclosing at least $\bar{N}$ out of $M$ data points, declare $\hat{\tau}_k^{(n)}$ as an interference MPC.
  - If there is more than one circle enclosing $\bar{N}$ or more data points, consider the circle enclosing maximum number of data points. If $X_n$ is outside the circle, declare $\hat{\tau}_k^{(n)}$ as an interference MPC and if $X_n$ is inside, declare $\hat{\tau}_k^{(n)}$ as a signal MPC.

Let $\Delta_n^I \triangleq \left\{\hat{\tau}_k^{(n)}, 1 \leq k \leq L_n \,|\, \hat{\tau}_k^{(n)} \text{is an interference MPC}\right\}$ be the collection of interference MPCs corresponding to the $n^{\text{th}}$ received waveform, $r_n(t)$. Similarly, the collection of signal MPCs is given by $\Delta_n^S \triangleq \left\{\hat{\tau}_k^{(n)}, 1 \leq k \leq L_n \,|\, \hat{\tau}_k^{(n)} \text{is a signal MPC}\right\}$.

*3) Interference suppression and noise averaging:* Notice that we could have stopped once $\hat{\tau}_k^{(n)}$ is detected as signal MPC. But doing so, we cannot take advantage of the increased SNR obtained from averaging the waveforms. Instead, we detect the interference MPCs, remove their contribution from the waveforms, and average them to increase the SNR.

$$\tilde{r}_n(t) = r_n(t) - \sum_{\hat{\tau} \in \Delta_n^I} \hat{h}_n(\hat{\tau}) p(t - \hat{\tau}), \ 1 \leq n \leq N. \quad (11)$$

Notice that the above steps remove strong interference and noise peaks. The waveforms are now averaged to suppress any weak residual interference and noise.

$$r_{\text{avg}}(t) = \frac{1}{N} \sum_{n=1}^{N} \tilde{r}_n(t). \quad (12)$$

*4) Range extraction:* Assuming that the interference is effectively suppressed in the above steps, $r_{\text{avg}}(t)$ can be treated as the received waveform in AWGN. We again use the CLEAN algorithm to extract the first MPC. To be fair in comparison, we chose the correlation threshold from the lookup table that is generated for $I = 0$ (No interference case). We furthermore require that the delay between the first and second MPC is consistent with the statistics of the inter-arrival times of MPCs, which is assumed to be known. This is required to filter out any residual interference MPCs, as their inter-arrival times has significantly larger delays than the signal MPCs. [2] When the MPC arrival times are modeled as Poisson process with parameter $\lambda$, probability that the inter-arrival times exceed $\frac{5.3}{\lambda}$ is $0.5\%$.

Let the extracted MPCs location be $\{\hat{\tau}_k, k \geq 1\}$. The ToA estimate is given by

$$\widehat{\text{ToA}} = \min \left\{ \hat{\tau}_k : |\hat{\tau}_k - \hat{\tau}_{k+1}| < \frac{5.3}{\lambda} \right\}. \quad (13)$$

## IV. Proposed algorithm analysis

We now analyze the performance of the proposed ranging scheme and study the impact of parameters $W$, $\gamma$ and $\bar{N}$. To make the analysis tractable we make the following modeling assumptions. The channel impulse responses of the users, $\{h_i(t)\}_{i=1}^{I+1}$, are assumed $i.i.d.$ random processes. For the $i^{\text{th}}$ user, the arrival times of the MPCs are modeled as Poisson process with rate $\lambda$ and the strength of the MPCs are assumed to be independent Rayleigh RVs. The chip sequence $c_i(n)$ are assumed $i.i.d.$ across $n$ (waveform index) and $i$ (user index), and independent of the channel impulse responses.

Thus, the MPC arrival times corresponding to the delayed impulse response $h_i(t - c_i(n)T_c)$ also follow a Poisson process with rate $\lambda$, for different $i$ and $n$. Hence, the MPC arrival times corresponding to the sum interference, $h_I^{(n)}(t)$, follow a Poisson process with rate $\lambda I$, and is $i.i.d.$ across $n$.

Henceforth, we use the following notation: $f_X(x)$ shall denote the density function of RV $X$. $\mathcal{P}(A)$ and $\mathbf{E}[A]$ shall denote the probability and expectation of $A$ respectively. Similarly $\mathcal{P}(A|B)$ shall denote the conditional probability of $A$ given $B$.

### A. False alarms from a noise peak

We will now compute the probability that the algorithm falsely detects a noise peak from CLEAN as a signal MPC. Let $\tau$ be the MPC location corresponding to a noise peak. Without loss of generality, we assume that a noise peak of strength $X_1$ ($|X_1| > \mu$), occurs at $\tau$, in the first waveform.

[2] For instance, with $1\%$ false alarm probability and $I = 10$ interfering users, the residual interference MPC inter-arrival times are exponential with mean $\frac{100}{\lambda I} = \frac{10}{\lambda}$. But, the signal MPC inter-arrival times are exponential with mean $\frac{1}{\lambda}$.

The algorithm makes false detection of $\tau$ as a signal MPC, if at least $\bar{N}-1$ of the remaining $N-1$ waveforms have a noise peak in $[\tau-W,\tau+W]$ and there exists a circle of radius $\gamma$ enclosing at least $\bar{N}$ of these points, including $X_1$. The false alarm probability is upper bounded by

$$P_{f,N} \leq \sum_{m=\bar{N}}^{N} \min\Bigg(\Bigg[\binom{N-1}{m-1}\left(1-2W\exp\left(-\frac{\mu^2}{N_0}\right)\right)^{N-m} \times \left(2W\exp\left(-\frac{\mu^2}{N_0}\right)\right)^{m-1}\Bigg], \Bigg[\sum_{k=\bar{N}}^{m} k\binom{m-1}{k-1}\int_0^{\infty}\frac{1}{N_0}\exp\left(-\frac{y}{N_0}\right) \times \left(1-Q_1\left(\sqrt{\frac{2y}{N_0}},\sqrt{\frac{2\gamma^2}{N_0}}\right)\right)^{k-1} Q_1\left(\sqrt{\frac{2y}{N_0}},\sqrt{\frac{2\gamma^2}{N_0}}\right)^{m-k} dy\Bigg]\Bigg),$$

where $Q_1(.,.)$ is the Marcum Q-function. The details are given in Appendix A.

### B. False alarms from an interference MPC

We will now compute the probability that the algorithm falsely detects an interference MPC as a signal MPC. Without loss of generality, we assume that an interference MPC of strength $X_1$ ($|X_1| > \mu$) occurs at $\tau$, in the first waveform. Let $E_I$ be the average energy of the interference MPCs.

The algorithm makes false detection of $\tau$ as a signal MPC if at least $\bar{N}-1$ of the remaining $N-1$ waveforms have an interference MPC in $[\tau-W,\tau+W]$ and there exists a circle of radius $\gamma$ enclosing at least $\bar{N}$ of these points, including $X_1$. The false alarm probability is upper bounded by

$$P_{f,I} \leq \sum_{m=\bar{N}}^{N} \min\left(\left[\binom{N-1}{m-1}\left(1-\exp\left(-2WI\lambda\right)\right)^{m-1} \times\exp\left(-2WI(N-m)\lambda\right)\right], \left[\sum_{k=\bar{N}}^{m} k\binom{m-1}{k-1}\int_0^{\infty}\frac{1}{E_I}\exp\left(-\frac{y}{E_I}\right) \times \left(1-Q_1\left(\sqrt{\frac{2y}{E_I}},\sqrt{\frac{2\gamma^2}{E_I}}\right)\right)^{k-1} Q_1\left(\sqrt{\frac{2y}{E_I}},\sqrt{\frac{2\gamma^2}{E_I}}\right)^{m-k} dy\right]\right).$$

The details are given in Appendix B.

### C. Signal MPC detection

Consider a signal MPC with strength $\alpha$ and at location $\tau$. We will now compute the probability that the algorithm detects $\tau$ as a signal MPC.

The algorithm correctly detects $\tau$ as a signal MPC, if in at least $\bar{N}$ of the $N$ waveforms $\tau$ is detected as MPC and there exists a circle of radius $\gamma$ enclosing at least $\bar{N}$ of these points. The detection probability is lower bounded by

$$P_d \geq \sum_{m=\bar{N}}^{N}\sum_{k=0}^{N-m}\sum_{l=\bar{N}}^{m}\binom{N}{m+k}\binom{m+k}{m}\binom{m-1}{l-1}p(\alpha)^m \times\left(1-p(\alpha)\right)^k\exp(-2W\lambda I(m+k))\left(1-\exp\left(-2W\lambda I\right)\right)^{N-m-k} \times\int_{\max(\mu-|\alpha|,0)}^{\infty} q(\alpha,r)^{l-1}\left(1-q(\alpha,r)\right)^{m-l}\frac{r}{\pi N_0}\exp\left(-\frac{r^2}{N_0}\right)g(r)dr,$$

where $p(\alpha)$ and $q(\alpha,r)$ are given in (26) and (29) respectively, $g(r)$ is defined in Appendix C. The details are given in Appendix C.

### D. Choice of parameters $\bar{N}$, $\gamma$, and $W$

From the analysis presented in the earlier section, it can be seen that as $\bar{N}$ increases, the false alarm from noise and interference decreases, but the signal MPC detection probability also decreases. Similarly as $\gamma$ or $W$ increases, the detection probability increases but the false alarms from noise and interference also increases. An optimized choice could be done based on the bounds derived above; however this would require a 3-dimensional grid search. We instead use a heuristic approach to find a good choice of parameters, and then use the bounds to demonstrate the effectiveness of these choices.

Probability of a noise peak occurring in the interval $[\tau-W,\tau+W]$, in any waveform is upper bounded using (19). Since noise in different waveforms is $i.i.d.$, the expected number of waveforms with a noise peak in the interval $[\tau-W,\tau+W]$ is upper bounded by

$$\mathbf{E}\left[\#\text{waveforms with a noise peak in } [\tau-W,\tau+W]\right] \leq 2WN\exp\left(-\frac{\mu^2}{N_0}\right). \quad (14)$$

Hence, we chose $\bar{N} \geq 2WN\exp\left(-\frac{\mu^2}{N_0}\right)$, so that the false alarms from noise peak is small.

Probability of an interference MPC in the interval $[\tau-W,\tau+W]$, in any waveform is $1-\exp\left(-2W\lambda I\right)$. Since interference MPC arrival times in different waveforms is $i.i.d.$, the expected number of waveforms with an interference MPC in the interval $[\tau-W,\tau+W]$ is given by

$$\mathbf{E}\left[\#\text{waveforms with an interference MPC in } [\tau-W,\tau+W]\right] = N\left(1-\exp\left(-2WI\lambda\right)\right). \quad (15)$$

Hence, we chose $\bar{N} \geq N\left(1-\exp\left(-2WI\lambda\right)\right)$, so that the false alarms from interference is small.

Consider a signal MPC with strength $\alpha$ and at location $\tau$. The expected number of waveforms in which an interference MPC also happens in $[\tau-W,\tau+W]$ is given by (15). Hence, on average only $N\exp\left(-2WI\lambda\right)$ waveforms are free from interference at $\tau$. For these waveforms free from interference, the estimated strength of the signal MPC at $\tau$ is $X_k = \alpha + N_k$. The radius of the circle, $\gamma$, is chosen such that with high probability, circle centered around one point encloses the other points. Since $|X_i - X_j|^2 = |N_i - N_j|^2$ is an exponential RV with mean $2N_0$, for $\gamma^* = 3\sqrt{N_0}$, we have

$$\mathcal{P}\left(|X_i - X_j| > \gamma^*\right) = \mathcal{P}\left(|N_i - N_j|^2 > 9N_0\right) = 0.01.$$

Also, we chose $\bar{N} \leq N\exp\left(-2WI\lambda\right)$, so that the probability of detection of signal MPC is high. Since the miss detection of signal MPC is more critical than the false alarms, as the false alarms can be further suppressed by steps 3 and 4 of the

algorithm, we chose

$$\bar{N}^* = \min\left[N\exp\left(-2WI\lambda\right), \max\left(2WN\exp\left(-\frac{\mu^2}{N_0}\right), N\left(1-\exp\left(-2WI\lambda\right)\right)\right)\right]. \quad (16)$$

The window size, $W$, should be small enough that the false alarms from a noise peak and an interference MPC is small. On the other hand it must be large enough that signal MPC is detected. We chose $W$ such that any signal MPC location estimate, obtained from CLEAN, is at most $W$ samples away from the true location. Setting 95% confidence interval for $\alpha = \mu$, in (10), we have

$$\mathcal{P}(|\tau - \hat{\tau}| \geq W^*) = Q\left(\sqrt{\frac{\mu^2}{N_0}\left(1 - R_p(2W^*)\right)}\right) = 0.05. \quad (17)$$

Using $\mu = 2.12\sqrt{N_0}$, we have $W^* = 0.5R_p^{-1}(0.4)$.

We now study the bounds developed on the false alarm and detection probability for the above choice of parameters. Figure 3 plots the false alarm probability $P_{f,N}$ and $P_{f,I}$ as a function of $E_I$ and the signal MPC detection probability $P_d$ as a function of $|\alpha|^2$. Performance is shown for $I = 1$, 5, and 10. It can be seen that the algorithm successfully rejects strong interference MPCs and also rejects the noise peaks significantly. Weak residual interference MPCs can be further suppressed by steps 3 and 4 of the algorithm. The signal MPC detection probability increases with $|\alpha|^2$. When the number of interfering users is large, an interference MPC overlaps with the signal MPC in several of the waveforms, and if the interference is strong, it makes the desired signal unrecognizable and hence the algorithm misses the signal MPCs. For $I = 10$, the signal MPC detection probability is only 0.55. In Figure 4, we justify the choice of parameters $(W^*, \gamma^*, \bar{N}^*)$. For $I = 5$, we plot the performance with significantly different choice of parameters. The solid lines is the performance with $(W, \gamma, \bar{N}) = \left(\frac{W^*}{3}, \frac{\gamma^*}{3}, \frac{\bar{N}^*}{3}\right)$. It has higher false alarms from noise and lower detection probability than $(W^*, \gamma^*, \bar{N}^*)$. The dotted lines is the performance with $(W, \gamma, \bar{N}) = (2W^*, 2\gamma^*, 2\bar{N}^*)$. It has very poor signal MPC detection probability.

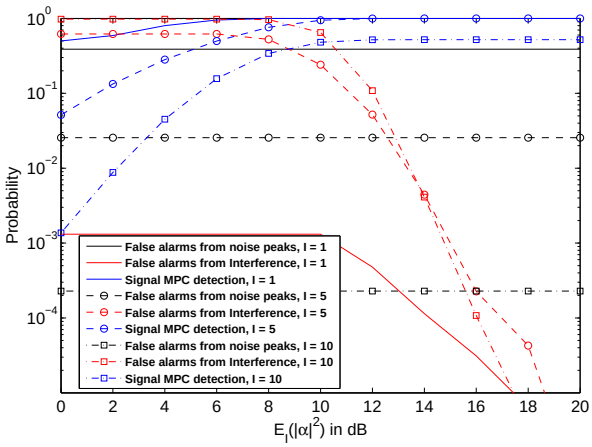


Fig. 3. Performance bounds with $(W^*, \gamma^*, \bar{N}^*)$ for $N = 50$ and $\lambda = 6$ ns.

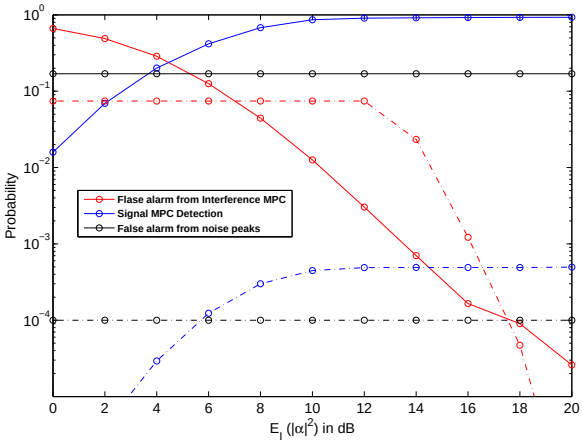


Fig. 4. Performance bounds with $(W, \gamma, \bar{N}) = \left(\frac{W^*}{3}, \frac{\gamma^*}{3}, \frac{\bar{N}^*}{3}\right)$ and $(W, \gamma, \bar{N}) = (2W^*, 2\gamma^*, 2\bar{N}^*)$ for $N = 50$, $I = 5$ and $\lambda = 6$ ns.

## V. Performance Evaluation with Synthetic Channels

We now evaluate the performance of the proposed ranging scheme and compare it with some of the well-studied schemes in the literature. The root mean square error (RMSE) in the distance, $\sqrt{\mathbf{E}\left[\left|\hat{d} - d\right|^2\right]}$, is used as the performance metric. Here $d$ is the true distance between the desired user and the receiver, and $\hat{d} \triangleq c\widehat{\text{ToA}}$ is the estimated distance with $c = 3 \times 10^8$ being the speed of light.

The following parameter settings were used. For the transmit pulse, the second derivative of the basic Gaussian pulse, $p(t) \propto \left(1 - 4\pi\left(\frac{t}{T_p}\right)^2\right)\exp\left(-2\pi\left(\frac{t}{T_p}\right)^2\right)$ is used with $T_p = 1$ ns. The parameters of the time-hopping signal are $T_c = 4$ ns and $N_c = 60$ ($T_f = N_c T_c = 240$ ns). The chip sequences $c_i(n)$ are generated $i.i.d.$ from the set $\{0, 1, \cdots, N_c - 1\}$ with equal probability. The performance was evaluated with $10^3$ channel realizations of the IEEE 802.15.4a CM1 (residential line-of-sight) channel model [2]. For each channel realization, the chip sequences of the $I + 1$ users and hence the corresponding time-hopping signals are regenerated independently. Three different values of $I$ ($I = 1$, $I = 5$ and $I = 10$) and two different values of $N$ ($N = 50$ and $N = 15$) were considered; $1/\lambda = 6$ ns was used. The window size using (17) was $W = 0.25$ ns (10 samples). $\bar{N}$ and $\gamma$ are chosen as per the discussion in Sec. IV-D. The performance of the proposed ranging scheme is compared with the thresholding schemes described in Sec. III-A and the non-linear filtering based energy detection schemes in [25]: for the minimum and median filtering, the performance is optimized over the block energy threshold and the length of the filter; the search back window size is fixed to 60 ns. We first present the results with interference from different users being the same. For the later part of simulations, we also model the path loss and shadowing and hence different SIR from different

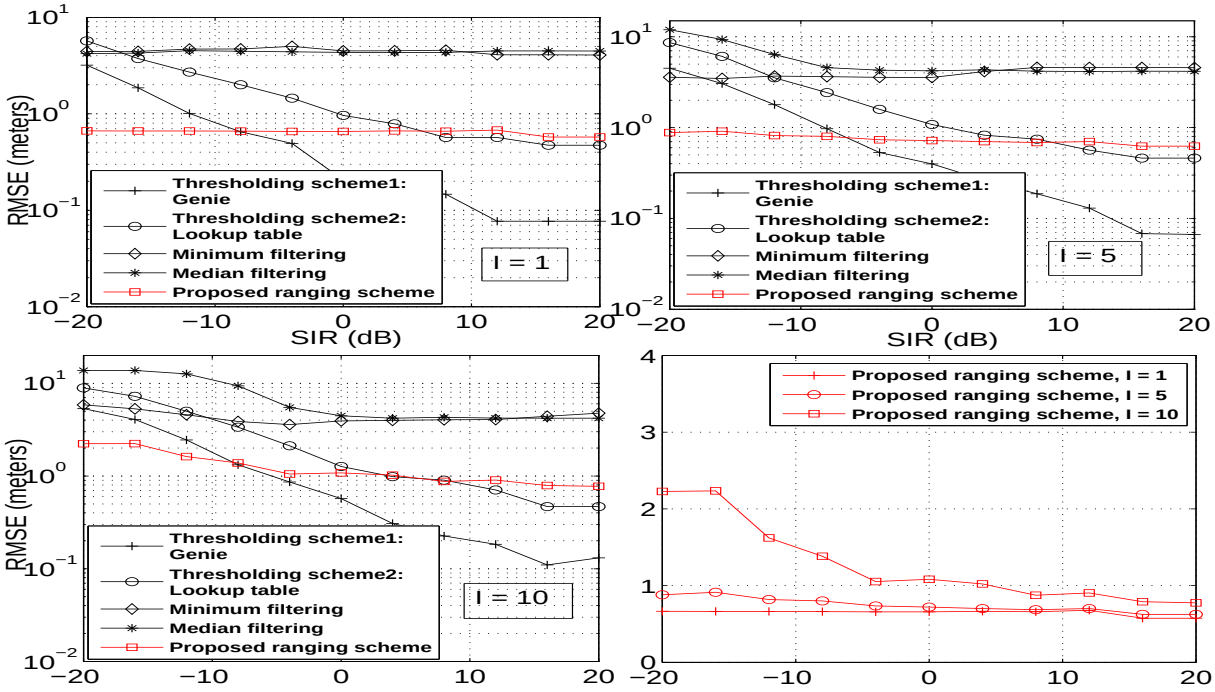


Fig. 5. Performance evaluation of different ranging schemes, as a function of SIR (SNR = 20 dB and $N = 50$).

interfering users.

Figure 5 compares the RMSE of different ranging schemes, as a function of SIR, for a fixed SNR of 20 dB and $N = 50$ waveforms. Performance was shown for $I = 1$, $I = 5$ and $I = 10$. From (16), the corresponding $\bar{N}$ are 12, 17, and 22. As mentioned earlier, we assume $E_2 = E_3 = \cdots = E_{I+1}$. As expected, for the thresholding schemes, the RMSE decreases with SIR. Also, for these schemes, RMSE significantly increases with $I$ in the interference limited regime. In the interference limited regime, the residual interference after averaging is comparable to the strength of the LOS component from the desired user and hence even a genie thresholding scheme has a large RMSE. The proposed ranging scheme effectively suppresses the strong interference MPCs (can also be seen from Figure 3), and hence reduces the RMSE significantly, and performs equally well at all SIR.

Notice that the proposed ranging scheme is always better than the minimum and median filtering schemes, is better than the lookup table thresholding scheme for SIR $\leq 8$ dB, and is even better than the genie thresholding scheme for SIR $\leq -8$dB. In the noise limited regime, averaging is the best thing to do and hence the lookup table thresholding scheme is slightly better than the proposed ranging scheme. While the proposed ranging scheme can eliminate noise peaks, it also misses weak signal MPCs resulting in increased RMSE. Also evident is the robustness of the proposed ranging scheme to the strength of the interference and the number of interfering users. While the RMSE is very similar for $I = 1$ and $I = 5$ in the interference limited regime, it slightly increases for $I = 10$. For large $I$, the proposed ranging scheme has a lower signal MPC detection probability as discussed in Figure 3, and hence increased RMSE.

Similar observations hold even for other values of $N$. For example, with $N = 15$ waveforms, the proposed ranging scheme is better than the lookup table thresholding scheme for SIR $\leq 10$ dB, it is better than even the genie thresholding scheme for SIR $\leq -4$ dB and is better than median and minimum filtering schemes at all SIR. The corresponding figure is not shown for lack of space. In general, smaller the $N$, better is the performance of the proposed ranging scheme relative to the thresholding schemes.

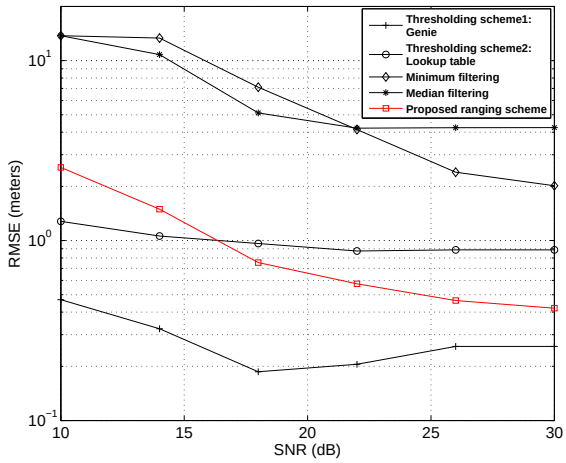


Fig. 6. Performance evaluation of different ranging schemes, as a function of SNR, in presence of one active interfering user (SIR = 0 dB, $I = 1$, and $N = 50$).

Figure 6 plots the RMSE of different ranging schemes as a function of SNR, for SIR $= 0$ dB and $I = 1$. As expected, the RMSE decreases with SNR for all the ranging schemes in the noise limited regime. When SNR is low (noise limited regime), averaging is better than any non-linear filtering and hence both the thresholding schemes outperform the proposed ranging

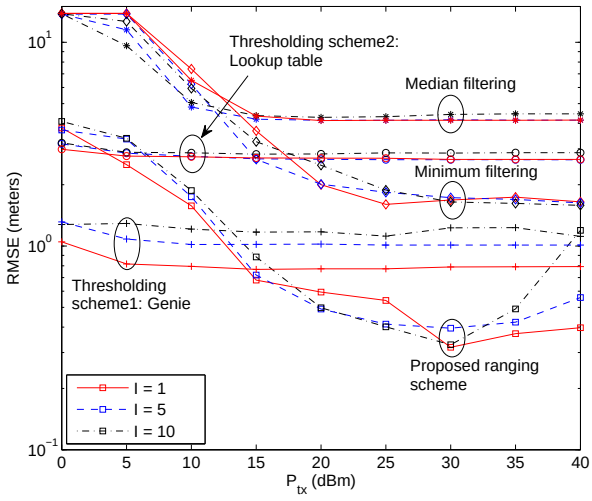


Fig. 7. Performance evaluation of different ranging schemes, as a function of transmit power, when SIR from different users is different ($N = 50$).

scheme. Beyond 16 dB SNR, interference is comparable to noise and hence the proposed ranging scheme perform better than the lookup table based thresholding scheme. However, it is still inferior to the genie scheme, which can change threshold every channel realization. Please note that the genie scheme is unrealistic and is only used as a benchmark.

So far we had implicitly assumed that all the interfering users are at same distance from the receiver and hence cause same interference. We now model the user locations using Poisson point process in two dimensional plane. The path loss and shadowing are modeled as per the specifications in IEEE 802.15.4a CM1 channel model. We assume all the users (both desired and interfering) transmit with the same power level $P_{tx}$. Since different interfering users are at different distance from the receiver, the received power from the interfering users $\left(E_k \propto P_{tx} d_k^{-n}\right)$ is different for different $k$.

Figure 7 compares the RMSE with different ranging schemes as a function of $P_{tx}$ and for different $I$. Notice that as $P_{tx}$ increases, the SNR increases but SIR remains the same. For small $P_{tx}$, the system is in noise limited regime and hence the ranging error decreases with $P_{tx}$. As mentioned earlier, in noise dominated regime, averaging is better than non-linear filtering and hence the thresholding schemes perform better than the proposed ranging scheme. Beyond certain $P_{tx}$, the system is in the interference limited regime and hence the performance does not change with $P_{tx}$ for the thresholding schemes. However for the proposed scheme, which can suppress the interference, the ranging error decreases with $P_{tx}$. Notice that the proposed scheme is better than lookup table thresholding scheme beyond $P_{tx} = 5$ dBm, is also better than the genie thresholding scheme for $P_{tx} \geq 15$ dBm, and is always better than the minimum and median filtering schemes. For large $P_{tx}$, the RMSE with the proposed ranging scheme slightly increases and this is more significant for $I = 10$. This can be explained as follows: For large $I$ and large $P_{tx}$, the strength of interference is large. Hence, as discussed earlier, interference MPC overlaps with signal MPC in most of the waveforms, and since interference is strong, it makes the desired signal unrecognizable and hence the algorithm misses the signal MPCs. Also the behaviors of the minimum and median filtering are consistent with the earlier work in the literature. At low SNR, median filtering is better and at high SNR, minimum filtering is better which is also reflected in the figure. Minimum filtering works well at high SNR and hence for large $P_{tx}$, it has lower RMSE than the lookup table thresholding scheme.

## VI. Measurement Setup and Results

### A. Measurement Site

The measurements were performed for both line-of-sight (LOS) and non-line-of-sight (NLOS) scenarios in an outdoor campus environment, namely the Vivian Hall of Engineering (VHE) building at USC. The LOS measurements were performed in the quad area, which is an open space enclosed by tall buildings and trees on all the four sides, making it a multipath rich environment. The terrain is a flat field mainly made up of 5 cm high grass. The transmitter was fixed and the receiver was moved around. Measurements were carried out with 3 sets of distances between Tx and Rx (20 m, 30 m, and 40 m). For each distance, the receiver was placed at 3 different positions (far apart) along the circumference of the circle with transmitter as the center. At every position, a virtual 1x4 SIMO antenna array, with horizontal separation of 10 cm was used at the receiver. The Tx/Rx antenna heights was set to 100 cm. The same procedure was repeated for the 8 NLOS receiver positions shown in Figure 8.

### B. Hardware and Post-processing

The channel measurements were performed with a UWB channel sounder. An arbitrary waveform generator (AWG) that can generate signals up to 12 GHz with a sampling rate of 24 GS/s is used at transmitter. A digital sampling scope (DSO) operating at 40 GS/s is used at receiver for data acquisition. The transmitter and receiver were synchronized using a trigger signal. A pair of UWB Skycross Omni-directional antennas was used at transmitter and receiver. The transmitter sends several repetitions of a multitone OFDM-like waveform, $p(t)$, continuously. The transmitted waveform has a frequency range of 3 GHz – 10 GHz with a center frequency of 6.5 GHz. The frequency band is divided into 9559 sub carriers with a uniform spacing of 732.42 KHz. Each waveform is 1.36 $\mu$s long and we store $N = 50$ such waveforms at the DSO for every measurement. We also record 3.45 $\mu$s of receiver noise (transmitter off) for every measurement. This is used to compute the noise power, $N_0$, and to set the parameters during the post processing. More details about the hardware and the excitation signal can be found in [10].

Since the measurements were conducted close to campus buildings with WiFi access points and devices, there was significant interference. The received signal is thus first passed through a band pass filter to remove the out of band interference. The template signal for the CLEAN algorithm was obtained from a measurement taken with the setup in the anechoic chamber at USC, with a known distance between

transmitter and receiver and thus includes the distortions by the antennas.

The time-hopping signal is obtained from the multitone received signal as follows: Let $y_k(t)$ be the filtered received signal for a receiver at position $k$. It is divided into $N$ disjoint intervals, each of $T_f = 1.36$ $\mu$s long. Let the resulting waveforms be $\left\{y_k^{(n)}(t)\right\}_{n=0}^{N-1}$. The time-hopping signal is obtained by introducing a shift to each of the $N$ waveforms and adding them back together.

$$y_k^{TH}(t) = \sum_{n=0}^{N-1} y_k^{(n)}(t - nT_f - c_k(n)T_c), \qquad (18)$$

where $c_k(n) \in \{0, 1, \cdots, 127\}$ is the chip sequence assigned to receiver at position $k$ and $T_c = \frac{T_f}{128}$ is the chip duration. $c_k(n)$ is generated $i.i.d.$ from the set $\{0, 1, \cdots, 127\}$.

Since only one AWG and one DSO were used in the measurements, the MUI is simulated by adding the measurements taken at different receiver positions. Since the transmitter location is same for all the measurements, assuming that the channel is reciprocal, this has the same effect as if multiple users were transmitting at the same time. For instance, $I = 3$ level MUI can be simulated by adding the time-hopping received waveforms at positions 5, 6 and 7 as interference to the time-hopping received waveform at position 1.

### C. Performance Evaluation with Measurement Data

We now evaluate the performance of the proposed ranging scheme with the measurement data, and compare it with the two thresholding schemes. For the performance evaluation with the proposed scheme, $\gamma^*$ and $W^*$ are chosen according to the discussion in Sec. IV-D. Assuming that no knowledge of $I$ was available, $\bar{N} = 0.02W^*N$ and $\bar{N} = \frac{N}{2}$ are used for AWGN ($I = 0$) and MUI respectively. For the lookup table thresholding scheme, the optimal threshold for LOS/NLOS scenarios is computed as follows: For every receiver position, the SNR and SIR are computed by averaging over the small scale fading and the Monte Carlo simulations were performed for these parameter settings and with CM5 (outdoor LOS)/CM6 (outdoor NLOS) channel models. The correlation threshold, $\eta$, with the minimum RMSE is picked. Since the transmitted pulse $p(t)$ is a long multi-tone waveform, the energy based non-coherent schemes suffer from poor SNR and hence the corresponding performance curves are not shown. The channel impulse response can also be computed from the channel transfer function and by applying a threshold, the noise and interference can be separated from the ToA of the desired user. The performance with this approach is not included as it is inferior to the thresholding schemes.

Figure 9 compares the CDF of the ranging error, $(\hat{d} - d)$, for different ranging schemes [3], when both the desired user and interfering users are in LOS scenario. Results are shown

[3]Please note that the setup here is very similar to the simulation setup used for Fig. 7, where the SIR from different users can be different. While Fig. 7 plots the RMSE as a function of transmit power, for the measurements we only plot the CDF of the ranging error as all the measurements were taken for a fixed transmit power.

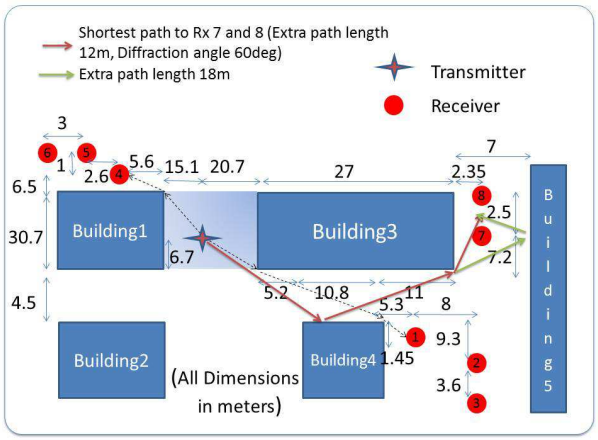


Fig. 8. NLOS measurement floor map of USC VHE quad.

for $I = 0$ (No MUI), 1, 5, and 8. In the absence of MUI, the ranging errors have a negative bias. This is because the threshold is chosen conservatively so as to minimize the RMSE, thereby resulting in higher early false alarms from noise peaks. While the proposed ranging scheme has slightly more RMSE than the lookup table thresholding scheme for $I = 0$ [4], it gives significantly lower RMSE than the lookup table thresholding scheme in the presence of MUI. While the ranging error with the proposed scheme is always less than 0.5 m, it is more than 20 m for 10% of times with the lookup table thresholding scheme when $I = 5$. The large negative errors are because of the early false alarms from interference MPCs. While the proposed scheme is robust to the number of interfering users, the performance with the lookup table thresholding scheme degrades as $I$ increases. Genie thresholding outperforms the other ranging schemes in this case.

Figure 8 gives the floor map of the NLOS measurement site with its dimensions. For these receiver locations, the direct path is completely blocked by the buildings. The only viable signal paths are diffractions around the corners of the buildings and reaching the receiver as shown. In the absence of MUI, the ranging errors (with both the proposed ranging scheme and the thresholding schemes) for the measurements taken at receiver positions 1–6 was less than 5 m. But for the measurements taken at receiver positions 7 and 8, it was 18–20 m. As shown in the figure, for the receiver positions 7 and 8, the shortest measurable signal path is the reflection from building 4, followed by diffraction at building 3. This path length is 12 m larger than the Euclidean distance between transmitter and receiver. However, the diffraction angle at building 3 is 60 degrees. Hence, the ray undergoes significant loss from diffraction and the corresponding MPC is not detectable. The next shortest path is from double reflection at buildings 4 and 5 as shown in Figure 8. This path length is 18 m more than the Euclidean distance. Since the RMSE is dominated by receiver positions 7 and 8, we exclude the corresponding measurements for the performance comparison of different ranging schemes. Results including these receiver positions are given in [5].

[4]The measured RMSE of 0.12 m is comparable (though slightly higher) than 0.08 m which is reported in [28].

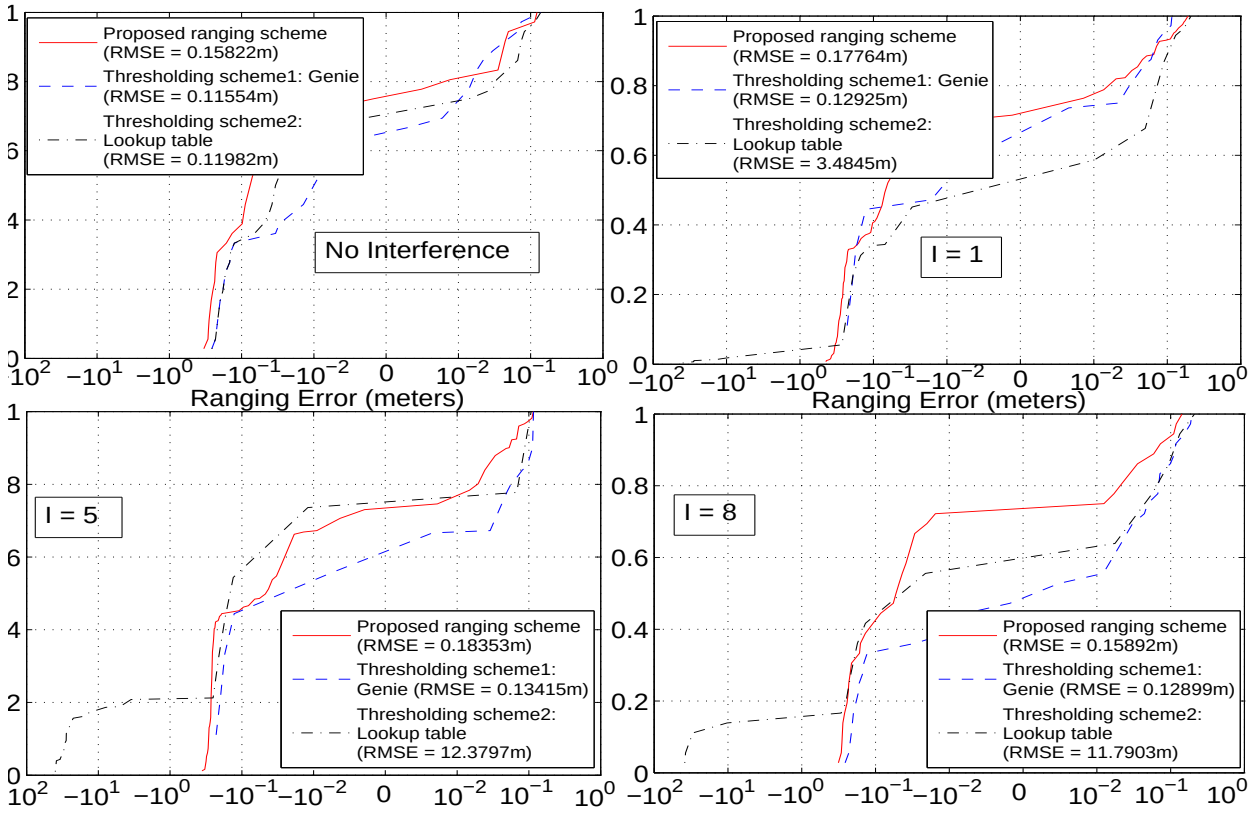


Fig. 9. Ranging error comparison for different schemes, when both desired and interfering users are in LOS scenario ($N = 50$).

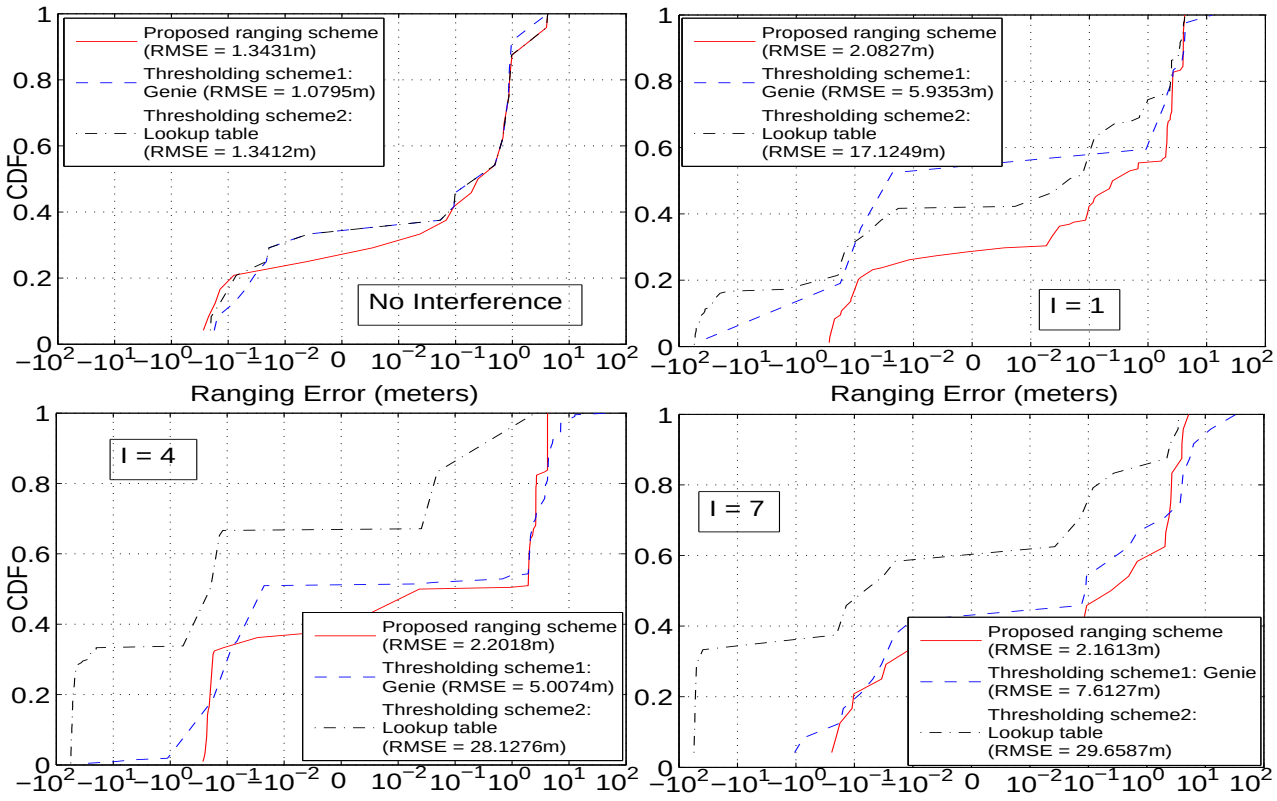


Fig. 10. Ranging error comparison for different schemes, when both desired and interfering users are in NLOS scenario ($N = 50$).

Figure 10 compares the CDF of the ranging error for different ranging schemes, when both the desired user and interfering users are in the NLOS scenario. In the AWGN channel (no MUI), all the three schemes have positive bias in the ranging error, as the direct path is blocked by the buildings. The proposed ranging scheme is as good as the lookup table thresholding scheme. Even with just one interfering user, the proposed scheme gives considerably lower RMSE than both the thresholding schemes. While the ranging error with the proposed scheme is always less than 5 m, it can be more than 15 m with the thresholding schemes. While the proposed scheme is robust to the number of interfering users, the performance with the thresholding schemes degrades as $I$ increases. The impact of MUI is more significant in NLOS scenarios and even the genie thresholding scheme cannot suppress the MUI effectively.

## VII. Conclusions

In this paper, we proposed a novel coherent ranging algorithm to mitigate the MUI. We considered time-hopping impulse radio. We observed that after de-hopping the received signal, receiver effectively sees multiple waveforms in which signal MPC occurs at same location, but interference MPC location for different waveforms is different. Using this observation, we were able to separate the interference MPCs and hence remove their contribution from the received signal. We also derived the performance bounds with the proposed ranging scheme. Using the IEEE 802.15.4a CM1 channel model as well as measured data, we showed the robustness of the proposed ranging scheme to the strength of interference and the number of interfering users.

## VIII. Acknowledgements

We thank Hao Feng, Sundar Aditya and Rui Wang for their help with the measurements, Dr. Alan Willner for providing test and measurement equipment for initial measurements, Asher Voskoboinik, Salman Khaleghi, and Hao Huang for their help with the hardware components.

## Appendix

### A. False alarms from a noise peak

A noise peak occurs in the interval $[\tau - W, \tau + W]$, in the $k^{\text{th}}$ waveform ($k > 1$), if $|N_k(t)| > \mu$ for some $t \in [\tau - W, \tau + W]$. It can be upper bounded as

$$\begin{aligned}&\mathcal{P}\left(\text{Noise peak in } [\tau - W, \tau + W] \text{ in } k^{\text{th}} \text{ waveform}\right)\\ &= \mathcal{P}\left(\exists t \in [\tau - W, \tau + W], |N_k(t)| > \mu\right)\\ &\leq 2W\mathcal{P}\left(|N_k(t)|^2 > \mu^2\right) = 2W \exp\left(-\frac{\mu^2}{N_0}\right). \qquad (19)\end{aligned}$$

Since it is assumed that the noise peak happens in the first waveform, the algorithm makes false detection of $\tau$ as a signal MPC, if at least $\bar{N} - 1$ of the $N - 1$ waveforms have a noise peak in $[\tau - W, \tau + W]$ and there exists a circle of radius $\gamma$ enclosing at least $\bar{N}$ of these points, including $X_1$. Let Event 1 $\triangleq$ $\{m - 1$ out of $N - 1$ waveforms have a noise peak in $[\tau - W, \tau + W]\}$ and Event 2 $\triangleq$ $\{\exists$ circle enclosing at least $\bar{N}$ of $m$ points, including $X_1\}$. The false alarm probability can be upper bounded by

$$\begin{aligned}P_{f,N} &\leq \sum_{m=\bar{N}}^{N} \mathcal{P}\left(\text{Event 1}, \text{Event 2}\right)\\ &\leq \sum_{m=\bar{N}}^{N} \min(\mathcal{P}\left(\text{Event 1}\right), \mathcal{P}\left(\text{Event 2}\right)). \qquad (20)\end{aligned}$$

Using (19), we have $\mathcal{P}\left(\text{Event 1}\right) \leq \binom{N-1}{m-1}\left(2W\exp\left(-\frac{\mu^2}{N_0}\right)\right)^{m-1}\left(1-2W\exp\left(-\frac{\mu^2}{N_0}\right)\right)^{N-m}$.

Let $X_1, X_2, \cdots, X_m$ be the strength of the $m$ noise peaks ($|X_i| > \mu$). Using union bound,

$$\begin{aligned}\mathcal{P}(\text{Event 2}) \leq &\sum_{l=1}^{m}\mathcal{P}\Big(\text{at least } \bar{N} \text{ of } m \text{ points, including } X_1,\\ &\text{enclosed by circle around } X_l\Big)\\ =&(m-1)\mathcal{P}\Big(\text{at least } \bar{N} \text{ of } m \text{ points, including } X_1,\\ &\text{enclosed by circle around } X_2\Big)\\ +&\mathcal{P}\big(\text{at least } \bar{N} \text{ of } m \text{ points are enclosed by circle around } X_1\big). \qquad (21)\end{aligned}$$

We will now evaluate each of the above two terms. The first term is given by

$$\begin{aligned}&\mathcal{P}\Big(\text{at least } \bar{N} \text{ of } m \text{ points, including } X_1,\\ &\quad\text{enclosed by circle with center } X_2 \text{ and radius } \gamma\Big)\\ &= \sum_{k=\bar{N}}^{m}\binom{m-2}{k-2}\mathcal{P}\Bigg(|X_1 - X_2| < \gamma, \prod_{j=3}^{k}|X_j - X_2| < \gamma,\\ &\qquad\qquad \prod_{j=k+1}^{m}|X_j - X_2| > \gamma\Bigg)\\ &= \sum_{k=\bar{N}}^{m}\binom{m-2}{k-2}\int \mathcal{P}\left(|X_1 - x_2| < \gamma\right)\prod_{j=3}^{k}\mathcal{P}\left(|X_j - x_2| < \gamma\right)\\ &\qquad\times \prod_{j=k+1}^{m}\mathcal{P}\left(|X_j - x_2| > \gamma\right) f_{X_2}(x_2)dx_2\\ &= \sum_{k=\bar{N}}^{m}\binom{m-2}{k-2}\int_0^{\infty}\left(1 - Q_1\left(\sqrt{\frac{2y}{N_0}}, \sqrt{\frac{2\gamma^2}{N_0}}\right)\right)^{k-1}\\ &\qquad\times Q_1\left(\sqrt{\frac{2y}{N_0}}, \sqrt{\frac{2\gamma^2}{N_0}}\right)^{m-k}\frac{1}{N_0}\exp\left(-\frac{y}{N_0}\right)dy, \qquad (22)\end{aligned}$$

where $Q_1(.,.)$ is the Marcum Q-function. We have used the fact that $\left\{|X_i|^2\right\}_{i=1}^{m}$ are $i.i.d.$ Exponential RVs with mean $N_0$ and $\{|X_i - x_2|\}_{i=3}^{m}$ are $i.i.d.$ Rice RVs with parameters $|x_2|$ and $\sqrt{\frac{N_0}{2}}$ [1]. The second term in (21) can similarly be

shown to be

$$\mathcal{P}\Big(\text{at least } \bar{N} \text{ of } m \text{ points are enclosed by circle with center } X_1 \text{ and radius } \gamma\Big) = \sum_{k=\bar{N}}^{m} \binom{m-1}{k-1} \int_0^\infty \left(1-Q_1\left(\sqrt{\frac{2y}{N_0}}, \sqrt{\frac{2\gamma^2}{N_0}}\right)\right)^{k-1} \times Q_1\left(\sqrt{\frac{2y}{N_0}}, \sqrt{\frac{2\gamma^2}{N_0}}\right)^{m-k} \frac{1}{N_0} \exp\left(-\frac{y}{N_0}\right) dy. \quad (23)$$

Using (22) and (23) in (21) and further using it in (20), the false alarm probability from a noise peak follows after some simplification.

### B. False alarms from an interference MPC

Interference peak occurs in the interval $[\tau - W, \tau + W]$, in the $k^{\text{th}}$ waveform ($k > 1$), if at least one interference MPC arrives in the interval $[\tau - W, \tau + W]$, and the strength of the interference exceeds the threshold $\mu$. Since $\mu$ is small, we assume that the strength of interference always exceeds threshold, whenever an interference MPC arrives in $[\tau - W, \tau + W]$. Hence, the probability of an interference peak is upper bounded by

$$\begin{aligned}&\mathcal{P}\big(\text{Interference peak in } [\tau-W,\tau+W], \text{ in the } k^{\text{th}} \text{ waveform}\big)\\ &\le \mathcal{P}\big(\text{at least one interference MPC arrives in } [\tau-W,\tau+W]\big)\\ &= 1-\exp\left(-2WI\lambda\right). \end{aligned} \quad (24)$$

We have used the fact that interference MPC arrivals are Poisson with parameter $\lambda I$. Since it is assumed that an interference peak happens in the first waveform, the algorithm makes false detection of $\tau$ as a signal MPC, if at least $\bar{N}-1$ of the $N-1$ waveforms has interference peak in $[\tau - W, \tau + W]$ and there exists a circle of radius $\gamma$ enclosing at least $\bar{N}$ of these points, including $X_1$. Let Event 1 $\triangleq$ $\{m-1$ out of $N-1$ waveforms has interference peak in $[\tau - W, \tau + W]\}$ and Event 2 $\triangleq$ $\{\exists$ circle enclosing at least $\bar{N}$ of $m$ points, including $X_1\}$. The false alarm probability is upper bounded by

$$\begin{aligned} P_{f,I} &\le \sum_{m=\bar{N}}^{N} \mathcal{P}\left(\text{Event 1}, \text{Event 2}\right)\\ &\le \sum_{m=\bar{N}}^{N} \min(\mathcal{P}\left(\text{Event 1}\right), \mathcal{P}\left(\text{Event 2}\right)). \end{aligned} \quad (25)$$

Using (24), we have $\mathcal{P}\left(\text{Event 1}\right) \le \binom{N-1}{m-1}(1-\exp\left(-2WI\lambda\right))^{m-1}\exp\left(-2WI(N-m)\lambda\right)$. Event 2 is very similar to the noise case, except that $\left\{|X_i|^2\right\}_{i=1}^{m}$ are now $i.i.d.$ Exponential RVs with mean $E_I$. Hence, replacing $N_0$ with $E_I$ in (22) and (23), and further using it in (25), the false alarm probability from an interference peak follows.

### C. Signal MPC detection

A signal MPC is detected in the interval $[\tau - W, \tau + W]$, in the $k^{\text{th}}$ waveform, if the offset in the location estimate by CLEAN is less than $W$ and the strength of the estimate, $X_k = \alpha + N_k$, exceeds the threshold $\mu$. The detection probability is given by

$$\begin{aligned} p(\alpha) &\triangleq \mathcal{P}\Big(\text{signal MPC is detected in } [\tau - W, \tau + W], \text{ in the } k^{\text{th}} \text{ waveform}\Big) \approx \mathcal{P}(|\tau-\hat{\tau}|\le W)\mathcal{P}(|X_k|>\mu)\\ &= \left(1-Q\left(\sqrt{\frac{|\alpha|^2}{N_0}(1-R_p(2W))}\right)\right) Q_1\left(\sqrt{\frac{2\,|\alpha|^2}{N_0}}, \sqrt{\frac{2\mu^2}{N_0}}\right). \end{aligned} \quad (26)$$

For some of the waveforms, an interference MPC can overlap with the signal MPC at $\tau$. Let Event 1$\triangleq$ {No interference in $[\tau - W, \tau + W]$, in $m+k$ out of $N$ waveforms}, Event 2$\triangleq$ {Signal MPC detected in $[\tau - W, \tau + W]$, in $m$ out of $m+k$ waveforms}, and Event 3$\triangleq$ $\{\exists$ circle enclosing at least $\bar{N}$ out of $m$ points$\}$. We assume that interference is strong enough that the resulting MPC estimates at $\tau$ in these waveforms are far away from true value, $\alpha$, and hence will be outside the circle. Hence the detection probability is lower bounded by

$$\begin{aligned} P_d &\ge \sum_{m=\bar{N}}^{N} \sum_{k=0}^{N-m} \mathcal{P}\left(\text{Event 1,Event 2,Event 3}\right)\\ &= \sum_{m=\bar{N}}^{N} \sum_{k=0}^{N-m} \mathcal{P}\left(\text{Event 1}\right) \mathcal{P}\left(\text{Event 2}|\text{Event 1}\right) \times \mathcal{P}\left(\text{Event 3}|\text{Event 1}, \text{Event 2}\right). \end{aligned} \quad (27)$$

Using (24), we have $\mathcal{P}\left(\text{Event 1}\right) = \binom{\bar{N}}{m+k}\exp(-2W\lambda I(m+k))\left(1-\exp\left(-2W\lambda I\right)\right)^{N-m-k}$. Using (26), we have $\mathcal{P}\left(\text{Event 2}|\text{Event 1}\right) = \binom{m+k}{m} p(\alpha)^m\left(1-p(\alpha)\right)^k$. We will now evaluate the conditional probability term. Let $\left\{X_i \triangleq \alpha+N_i, 1\le i\le m\right\}$ be the strength of the $m$ detected MPCs that are free from interference. The conditional probability can be lower bounded as

$$\begin{aligned} &\mathcal{P}\left(\text{Event 3}|\text{Event 2}, \text{Event 1}\right) \ge \mathcal{P}\Big(\text{circle centered at } X_1 \text{ with radius } \gamma \text{ encloses at least } \bar{N} \text{ points} \,\Big|\, \text{Event 1}, \text{Event 2}\Big)\\ &= \sum_{l=\bar{N}}^{m} \binom{m-1}{l-1} \mathcal{P}\left(\prod_{j=2}^{l} |N_j - N_1| < \gamma, \prod_{j=l+1}^{m} |N_j - N_1| > \gamma \,\Big|\, |\alpha+N_1|>\mu, \cdots, |\alpha+N_m|>\mu\right)\\ &= \sum_{l=\bar{N}}^{m} \binom{m-1}{l-1} \int_{n_1:|\alpha+n_1|>\mu} \mathcal{P}\Big(|N-n_1|<\gamma \,\Big|\, |\alpha+N|>\mu\Big)^{l-1} \times \mathcal{P}\Big(|N-n_1|>\gamma \,\Big|\, |\alpha+N|>\mu\Big)^{m-l} f_{N_1}(n_1) dn_1. \end{aligned} \quad (28)$$

The conditional probability term in (28) can be written as $\mathcal{P}\Big(|N-n_1|<\gamma \,\Big|\, |\alpha+N|>\mu\Big) =$

$\mathcal{P}(|N-n_1|<\gamma, |\alpha+N|>\mu)\,\mathcal{P}\left(|\alpha+N|>\mu\right)^{-1}$. Since $N$ is a complex Gaussian RV with variance $N_0$, we have $\mathcal{P}\left(|\alpha+N|>\mu\right) = Q_1\left(\sqrt{\frac{2|\alpha|^2}{N_0}}, \sqrt{\frac{2\mu^2}{N_0}}\right)$. Since $\mu \triangleq 2.12\sqrt{N_0}$ is small, for $|\alpha|^2 >> N_0$, we have $\mathcal{P}(|N-n_1|<\gamma, |\alpha+N|>\mu) \approx \mathcal{P}(|N-n_1|<\gamma) = 1-Q_1\left(\sqrt{\frac{2|n_1|^2}{N_0}}, \sqrt{\frac{2\gamma^2}{N_0}}\right)$. Hence we have

$$q(\alpha,|n_1|) \triangleq \mathcal{P}\left(|N-n_1|<\gamma \,\middle|\, |\alpha+N|>\mu\right)$$
$$\approx \left(1-Q_1\left(\sqrt{\frac{2\,|n_1|^2}{N_0}}, \sqrt{\frac{2\gamma^2}{N_0}}\right)\right) Q_1\left(\sqrt{\frac{2\,|\alpha|^2}{N_0}}, \sqrt{\frac{2\mu^2}{N_0}}\right)^{-1}. \quad (29)$$

Note that $|N_1|$ is a Rayleigh RV and $\angle N_1$ is a uniform RV.

Rewriting the integral in (28) in polar coordinates and evaluating it over $\angle N_1$, we get

$$\iint_{r,\theta:\cos(\theta-\angle\alpha)>\frac{\mu^2-|\alpha|^2-r^2}{2r|\alpha|}} q(\alpha,r)^{l-1}\left(1-q(\alpha,r)\right)^{m-l} \frac{r}{\pi N_0}\exp\left(-\frac{r^2}{N_0}\right) dr d\theta$$
$$= \int_{\max(\mu-|\alpha|,0)}^{\infty} q(\alpha,r)^{l-1}\left(1-q(\alpha,r)\right)^{m-l} \frac{r}{\pi N_0}\exp\left(-\frac{r^2}{N_0}\right) g(r) dr, \quad (30)$$

where $g(r) = 2\cos^{-1}\left(\frac{\mu^2-|\alpha|^2-r^2}{2r|\alpha|}\right)$ for $r \in (|\mu-|\alpha||, |\alpha|+\mu)$ and is $2\pi$ otherwise.

Hence the detection probability follows.

## REFERENCES


[1] A. F. Molisch, *Wireless Communications*. New York: IEEE Press/Wiley, 2ed., 2011.

[2] A. F. Molisch, D. Cassioli, C. C. Chong, S. Emami, A. Fort, B. Kannan, J. Karedal, J. Kunisch, H. G. Schantz, K. Siwiak, and M. Z. Win, "A comprehensive standardized model for ultrawideband propagation channels," *IEEE Transactions on Antennas and Propagation*, vol. 54, no. 11, pp. 3151–3166, November 2006.

[3] P. Bahl and V. N. Padmanabhan, "RADAR: An In-Building RF-based User Location and Tracking System," *Proc. IEEE Conference on Computer Communications* (INFOCOM), 2000.

[4] B. Li, A. G. Dempster, J. Barnes, C. Rizos, and D. Li, "Probabilistic algorithm to support the fingerprinting method for CDMA location", *Int. Symp. On GPS/GNSS*, Hong Kong, 8-10 Dec. 2005.

[5] V. Kristem, S. Niranjayan, S. Sangodoyin, and A. F. Molisch, "Experimental Determination of UWB Ranging Errors in an Outdoor Environment", *to appear in ICC.*, 2014.

[6] M. Z. Win and R. A. Scholtz, "Impulse radio: How it works", *IEEE Commun. Lett.*, vol. 2, pp. 36–38, 1998.

[7] J. A. Hogbom, "Aperture Synthesis with a Non-Regular Distribution of Interferometer Baselines," *Astronomy and Astrophysics Supplement Ser.*, vol. 15, 1974.

[8] R. J. M.Cramer, R. A. Scholtz, M. Z. Win, "Evaluation of an Ultra-wide-Band Propagation channel," *IEEE Transactions on Antenna and Propagation*, Vol.50, no.5, pp.561–570, May 2002.

[9] Muqaibel, A.; Safaai-Jazi, A.; Woerner, B.; Riad, S.; "UWB channel impulse response characterization using deconvolution techniques," *45th Midwest Symposium on Circuits and Systems*, Volume 3, Aug. 2002.

[10] S. Sangodoyin, S. Niranjayan and A. F. Molisch, "Ultrawideband Near-Ground Outdoor Propagation Channel Measurements and Modeling," *in Proc. 7th EuCAP*, Gothenburg, Sweden. April 2013.

[11] H. L. Van Trees, "Detection, Estimation, and Modulation Theory", 1968 :*Wiley.*

[12] S. Bellini and G. Tartara, "Bounds on error in signal parameter estimation," *IEEE Trans. Commun.*, vol. 22, pp.340–342, 1974.

[13] D. Chazan , M. Zakai and J. Ziv, "Improved lower bounds on signal parameter estimation," *IEEE Trans. Inf. Theory*, vol.IT-21, pp.90–93 1975.

[14] J. Zhang , R. A. Kennedy and T. D. Abhayapala, "Cramer-Rao lower bounds for the synchronization of UWB signals," *EURASIP J. Wireless Commun. Netw.*, vol.3, 2005.

[15] D. Dardari, C. C. Chong, M. Z. Win, "Improved Lower Bounds on Time-of-Arrival Estimation Error in Realistic UWB Channels," *Proc. IEEE Int. Conf. Ultra-Wideband (ICUWB)*, pp.531–537 2006.

[16] M. Z. Win and R. A. Scholtz, "Characterization of ultra-wide bandwidth wireless indoor communications channel: A communication theoretic view," *IEEE J. Sel. Areas Commun.*, vol.20, pp.1613–1627 2002.

[17] H. Saarnisaari, "ML time delay estimation in a multipath channel," *Proc. IEEE Int. Symp. Software Test. Anal. (ISSTA)*, pp.1007–1011 1996.

[18] J. Y. Lee and R. A. Scholtz, "Ranging in a dense multipath environment using an UWB radio link," *IEEE J. Sel. Areas Commun.*, vol.20, pp.1677–1683 2002.

[19] C. Falsi , D. Dardari , L. Mucchi and M. Z. Win, "Time of arrival estimation for UWB localizers in realistic environments," *EURASIP J. Appl. Signal Process. (Special Issue on Wireless Location Technologies and Applications)*, pp.1–13 2006.

[20] I. Guvenc and Z. Sahinoglu, "Threshold-based TOA estimation for impulse radio UWB systems," *Proc. IEEE Int. Conf. Ultra-Wideband (ICUWB)*, pp.420–425 2005.

[21] I. Guvenc , Z. Sahinoglu , A. F. Molisch and P. Orlik, "Non-coherent TOA estimation in IR-UWB systems with different signal waveforms," *Proc. IEEE Broadband Netw. (BROADNETS)*, vol. 2, pp.1168–1174 2005.

[22] D. Dardari, A. Conti, U. Ferner, A. Giorgetti, M. Z. Win, "Ranging With Ultrawide Bandwidth Signals in Multipath Environments," *Proceedings of the IEEE*, vol.97, no.2, pp.404–426, Feb. 2009.

[23] S. Gezici, Z. Sahinoglu, A. F. Molisch, H. Kobayashi, and H. V. Poor, "Two-Step Time of Arrival Estimation for Pulse-Based Ultra-Wideband Systems," *EURASIP Journal on Advances in Signal Processing*,vol. 2008.

[24] A. Giorgetti and M. Chiani, "Time-of-Arrival Estimation Based on Information Theoretic Criteria," *Signal Processing, IEEE Transactions on*, vol.61, no.8, pp.1869–1879, Apr. 2013.

[25] Z. Sahinoglu and I. Guvenc, "Multiuser interference mitigation in noncoherent UWB ranging via nonlinear filtering," *EURASIP J. Wireless Commun. Netw.*, pp.1–10 2006.

[26] D. Dardari , A. Giorgetti and M. Z. Win, "Time-of-arrival estimation of UWB signals in the presence of narrowband and wideband interference," *Proc. IEEE Int. Conf. Ultra-Wideband (ICUWB)*, pp.71–76 2007.

[27] A. G. Amigo, A. Mallat, and L. Vandendorpe, "Multiuser and Multipath Interference Mitigation in UWB TOA Estimation," *Proc. IEEE Int. Conf. Ultra-Wideband (ICUWB)*, pp.465–469 2011.

[28] Yuan Zhou, C. L. Law, Jingjing Xia, Kee Siang Koh, "Long range UWB localization system: From design to measurement," *Proc. IEEE Int. Conf. Ultra-Wideband (ICUWB)*, pp.1–4 2010.


PLACE PHOTO HERE

**Vinod Kristem** received his Bachelor of Technology degree in Electronics and Communications Engineering from the National Institute of Technology (NIT), Warangal in 2007. He received his Master of Engineering degree in Telecommunications from the Dept. of Electrical Communication Engineering, Indian Institute of Science, Bangalore, India in 2009. From 2009–2011, he was with Beceem Communications Pvt. Ltd., Bangalore, India (which was recently acquired by Broadcom Corp.), where he worked on channel estimation and physical layer measurements for WiMAX and LTE. He is currently working toward his Ph.D. degree with the Department of Electrical Engineering, University of Southern California, Los Angeles. His research interests include the design and analysis of receiver algorithms for wireless communication networks, Antenna selection in MIMO systems, and cooperative localization in wireless networks.


**Andreas F. Molisch** (S'89-M'95-SM'00-F'05) received the Dipl. Ing., Ph.D., and habilitation degrees from the Technical University of Vienna, Vienna, Austria, in 1990, 1994, and 1999, respectively. He subsequently was with AT&T (Bell) Laboratories Research (USA); Lund University, Lund, Sweden, and Mitsubishi Electric Research Labs (USA). He is now a Professor of Electrical Engineering with the University of Southern California, Los Angeles.

His current research interests are the measurement and modeling of mobile radio channels, ultra-wideband communications and localization, cooperative communications, multiple-input-multiple-output systems, wireless systems for healthcare, and novel cellular architectures. He has authored, coauthored or edited four books (among them the textbook Wireless Communications, Wiley-IEEE Press), 16 book chapters, some 160 journal papers, and numerous conference contributions, as well as more than 70 patents and 60 standards contributions.

Dr. Molisch has been an Editor of a number of journals and special issues, General Chair, Technical Program Committee Chair, or Symposium Chair of multiple international conferences, as well as Chairman of various international standardization groups. He is a Fellow of the IEEE, Fellow of the AAAS, Fellow of the IET, an IEEE Distinguished Lecturer, and a member of the Austrian Academy of Sciences. He has received numerous awards, most recently the Donald Fink Prize of the IEEE, and the Eric Sumner Award of the IEEE.


**S Niranjayan** (S'03-M'10) received the B.Sc. Eng. degree with first class honors in electronic and telecommunication engineering from the University of Moratuwa, Sri-Lanka, in 2001, the M.Eng. degree in electrical engineering from the National University of Singapore (NUS), Singapore, in 2004, and the Ph.D. degree in electrical engineering from the University of Alberta, Edmonton, Canada in 2010. Dr. Niranjayan was a recipient of the National University of Singapore (NUS) graduate scholarship. He has been a recipient of the Alberta Ingenuity graduate student scholarship and the iCORE post graduate scholarship during 2006-2010. He also received the Natural Sciences and Engineering Research Council of Canada's (NSERC) postdoctoral fellowship award during 2011 and 2012. Since 2011 he has been a postdoctoral fellow at the University of Southern California, Los Angeles, CA.


**Seun Sangodoyin** received his B.Sc in Electrical Engineering from Oklahoma State University in May 2007, M.Sc in the same field at the University of Southern California (USC) in 2009, he is currently working toward his Ph.D in Electrical Engineering at the University of Southern California (USC). His research interest includes Measurement-based MIMO channel Modeling and analysis, UWB MIMO Radar, Parameter Estimation, Body area Networks and Stochastic dynamical Systems.